Paleontological Research, vol. 5, no. 1, pp. 33-44, April 30, 2001

Geometric pattern and growth rate of prismatic shell structures in Bivalvia

TAKAO UBUKATA

Institute of Geosciences, Shizuoka University, Oya 836, Shizuoka, 422-8529, Japan
(*sbtubuk@ipc.shizuoka.ac.jp*)

Received 11 October 2000; Revised manuscript accepted 27 November 2000

Abstract. The distribution patterns, sizes and nucleation sites of aggregated prisms on the outer shell surface were examined in 16 species of Bivalvia and modeled theoretically. Biometric analysis shows a negative correlation between the median size and variation of sizes of calcitic simple prisms. In species with aragonitic vertical composite prisms, instead, the density of prisms tends to decrease when their nucleation sites are randomly distributed. Comparison of the results of computer simulations with those of biometric analyses reveals the following: 1) a positive correlation between growth rate of prisms and the probability of nucleation for simple prisms, and 2) a limit of the number of nucleations per unit time in vertical composite prisms. Prism size correlates with the growth rate of the entire shell or prisms, and increases as the shell grows faster or prisms grow slower.

Key words: biomineralization, bivalves, prismatic structure, shell growth rate, theoretical morphology

Introduction

The microscopic features of a molluscan shell record certain physiological conditions of the organism at the time the shell is formed. Carbonate minerals within a molluscan shell crystallize and grow under physicochemical conditions controlled by the physiology of the organism. Wada (1972, 1985) reported a seasonal change of shape and size of aragonite crystals in the nacreous layer of such bivalves as *Pinctada fucata*, *Pinna attenuata* and *Hyriopsis schlegeli*. He suggested that the topography of growing crystals may reflect the rate of crystal growth or the degree of supersaturation of the extrapallial fluid. Quantitative analysis of the relationship between size and/or shape of crystals and the rate of crystal growth within a shell provides a reliable basis to understand the 'paleophysiology' of fossil organisms.

The goal of this study is to clarify the relationship between the geometry of bivalve shell microstructure and the relative growth rate of crystals or of the entire shell. For this purpose, the present study focuses on the geometry of the outer shell surface of a simple or vertical composite prismatic shell layer. Although they differ in the ultrastructure of prisms, those two prismatic structures both consist of many parallel-arrayed columnar units (Carter and Clark, 1985; Carter *et al.*, 1990). Each prism is surrounded and bounded by an organic matrix showing a honeycomb-like appearance on the outer shell surface.

For understanding the rule or algorithm forming the geometric pattern of shell microstructure, theoretical morphology is particularly useful (Ubukata, 1997a, b, 2000). In the present study, a biometric analysis of size and nucleation sites of prisms in actual shells was carried out in 16 species. Furthermore, a theoretical morphological modeling of growth kinematics of aggregated prisms was attempted, and the computer simulations of that model were compared with the results of the biometric analyses.

Biometric analyses

Material and methods

The outer shell surface of a simple prismatic or vertical composite prismatic outer shell layer was examined in 16 extant species of Bivalvia (Table 1). Each species was represented by a single specimen, except *Anodonta woodiana*. Most of them were collected at various localities around the Japanese Islands and the Philippines. All the specimens examined are stored at Shizuoka University (SUM).

In order to remove the periostracum from the shell completely, the shells examined were bleached for one day. Pieces of them were washed, dried in air, coated with gold using a JEOL JFC-1500 ion coater, and examined with a JEOL JSM-5800LV scanning electron microscope operated at 15kV and interfaced to a computer (Dell Optiplex Gxa EM).

In order to analyze size-frequency distribution of prisms,

Table 1. List of material examined. All specimens have the prefix SUM.

Family	species	locality	specimens
Pteriidae	*Pteria penguin* (Roding)	San Luice, Bathangas, Philippines	HM-B-0014
	Pinctada maculata (Gould)	Iriomote Is., Okinawa, southwest Japan	HM-B-0015
Isognomonidae	*Isognomon perna* (Linnaeus)	Iriomote Is., Okinawa, southwest Japan	HM-B-0016
	I. ephippium (Linnaeus)	San Luice, Bathangas, Philippines	HM-B-0017
Malleidae	*Malleus regula* (Forskål)	Iriomote Is., Okinawa, southwest Japan	HM-B-0018
Pinnidae	*Atrina pectinata* (Linnaeus)	Ariake, Saga, western Japan	HM-B-0019
	A. vexillum (Born)	Honda Bay, Palawan, Philippines	HM-B-0020
Ostreidae	*Crassostrea gigas* (Thunberg)	Misaki, Kanagawa, Central Japan	HM-B-0021
Margaritiferidae	*Margaritifera laevis* (Haas)	Nakagawa, Hokkaido, northern Japan	HM-B-0022
Unionidae	*Inversidens reiniana* (Kobelt)	Lake Biwa, Shiga, Central Japan	HM-B-0023
	Unio biwae Kobelt	Lake Biwa, Shiga, Central Japan	HM-B-0024
	Lanceolaria oxyrhyncha (Martens)	Lake Biwa, Shiga, Central Japan	HM-B-0025
	Anodonta woodiana (Lea)	Lake Biwa, Shiga, Central Japan	HM-B-0026, -0027
	A. calypygos Kobelt	Lake Biwa, Shiga, Central Japan	HM-B-0028
	Cristaria plicata (Leach)	Lake Biwa, Shiga, Central Japan	HM-B-0029
Trigoniidae	*Neotrigonia margaritacea* (Lamarck)	French Is., Australia	HM-B-0030

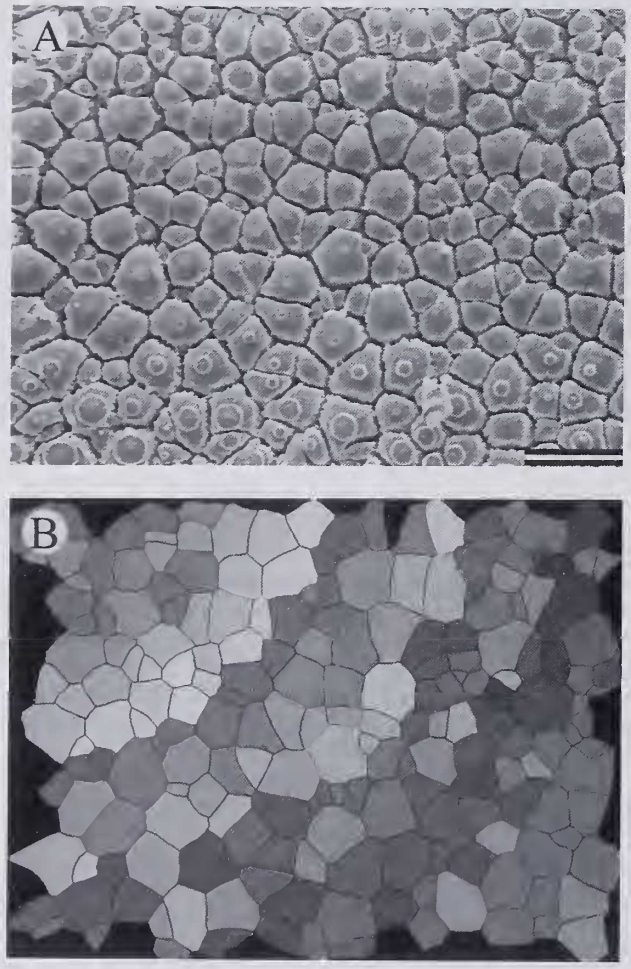

areas of prisms on the outer shell surface were measured at 6–12 positions along a growth increment on the shell surface. An SEM image of the measured portion was saved as a computer bitmap file (Figure 1A). Next, the boundaries between prisms were traced on a NEC PC-9821 V166 personal computer using Microsoft PowerPoint 7.0, and then each prism was colored differently using Justsystem Hanako PhotoRetouch (Figure 1B). Subsequently, the area of each prism was measured by counting pixels. For this counting, a program written in VISUAL BASIC was used on a personal computer.

Since the size-frequency distribution of the areas of prisms is generally right-skewed, the mean and standard deviation are not suitable for representing the distribution of the areas of prisms. Therefore, the "average" area of prisms on a shell is represented by the median of the areas ($\tilde{S}$), and the variation of the areas is expressed as a standardized hinge spread (Q_s), which is defined as follows:

$$Q_s \equiv \frac{Q_t - Q_f}{\tilde{S}}, \qquad (1)$$

where Q_f and Q_t are the first and third quartiles of the areas of prisms, respectively (Hoel, 1976). $\tilde{S}$ and Q_s were both estimated in all shell portions examined.

On the outer surface of a vertical composite prismatic shell layer, microgrowth increments are clearly visible within a bleached prism (Figure 2A). In a simple prismatic shell layer, growth increments within a prism are faintly observed on the bleached shell surface (Figure 2B). In either case,

Figure 1. **A.** SEM photograph of the outer shell surface of the vertical composite prismatic layer in *Anodonta woodiana* (SUM-HM-B0027), scale: 50 μm. **B.** Trace of the outlines of prisms on the SEM image of **A.**

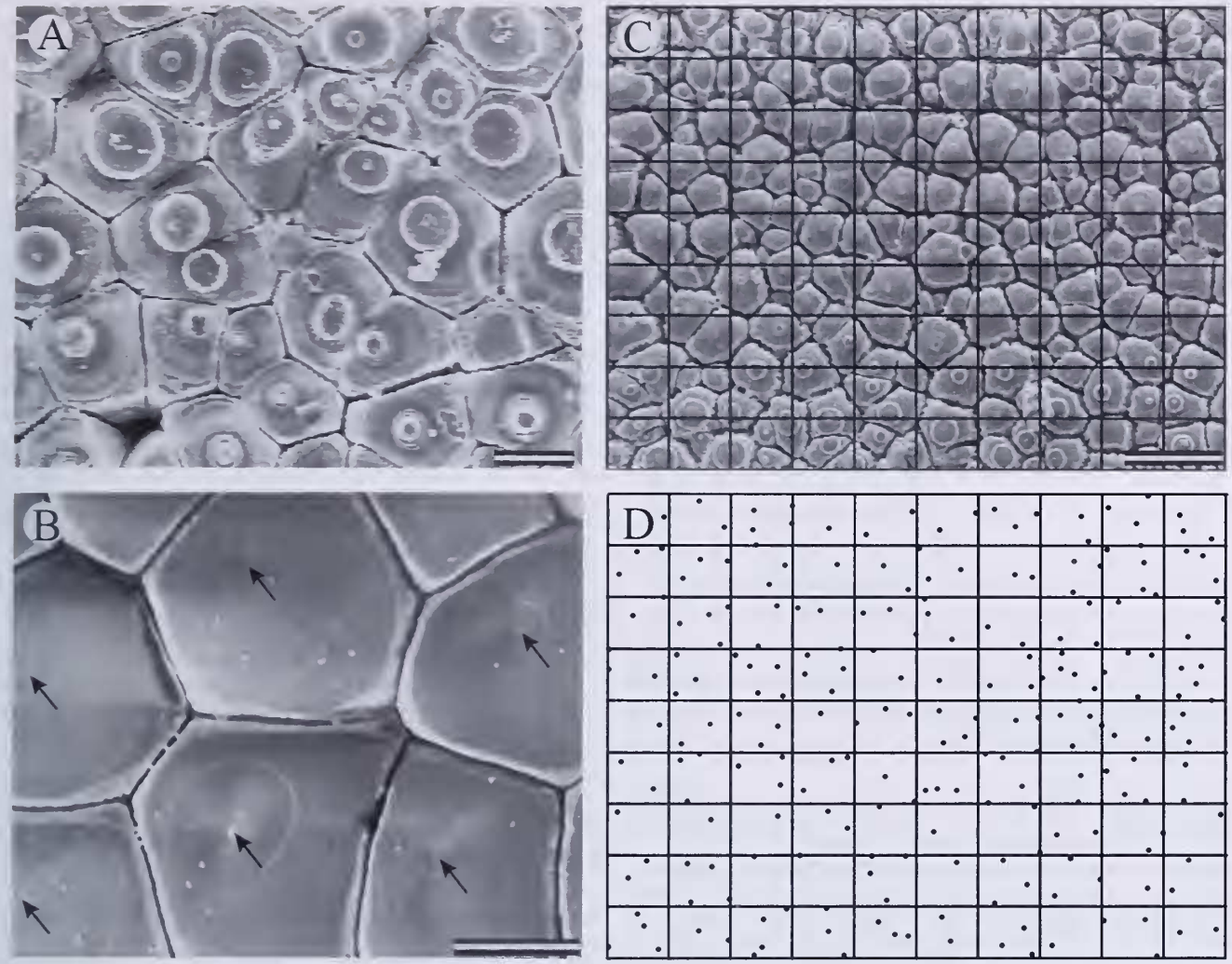

Figure 2. **A**. SEM photograph of the outer shell surface of the vertical composite prismatic shell layer in *A. woodiana* (SUM-HM-B0027) showing clear growth increments within individual prisms, scale: 20 μm. **B**. The simple prismatic layer in *Pinctada maculata* (SUM-HM-B0015). Arrows indicate nucleation sites, scale: 20 μm. **C**. The SEM image of *A. woodiana* subdivided into squares, scale: 50 μm. **D**. Distribution of nucleation sites of prisms in **C**.

the center of the circular growth increments is regarded as the nucleation site of the prism.

The distribution of nucleation sites of prisms was analyzed in all shell portions in which the areas of prisms were measured. An SEM image was divided into a squared grid of appropriate size for each square to include an average of two nucleation sites (Figure 2C). Next, the number of nucleation sites was counted in each square (Figure 2D). The numbers of squares and nucleation sites in each square both define the I_δ index of Morisita (1959), which represents the nonuniformity of a distribution independent of the size of the quadrates. The I_δ index is defined as:

$$I_\delta = \frac{n\sum_{i=1}^{n} x_i(x_i-1)}{\sum_{i=1}^{n} x_i\left(\sum_{i=1}^{n} x_i-1\right)}, \qquad (2)$$

where n is the number of squares, x_i is the number of sites in the square i. The value of I_δ is zero when the distribution is perfectly uniform (Figure 3A). I_δ increases as the distribution becomes nonuniform (Figure 3B), and it is expected to be one when sites are distributed randomly (Figure 3C). When the distribution of sites is biased considerably, I_δ has a large value (Figure 3D). The value of I_δ was estimated in every shell position examined, and the nonuniformity of the distribution of nucleation sites was represented by I_δ.

Results

The biometric analyses revealed a negative correlation between $\tilde{S}$ and Q_i in a single specimen of *Isognomon perna*, and a positive correlation in a single specimen of *Malleus regula* (Figure 4B). In another species, no correlation was observed, though the number of measured portions

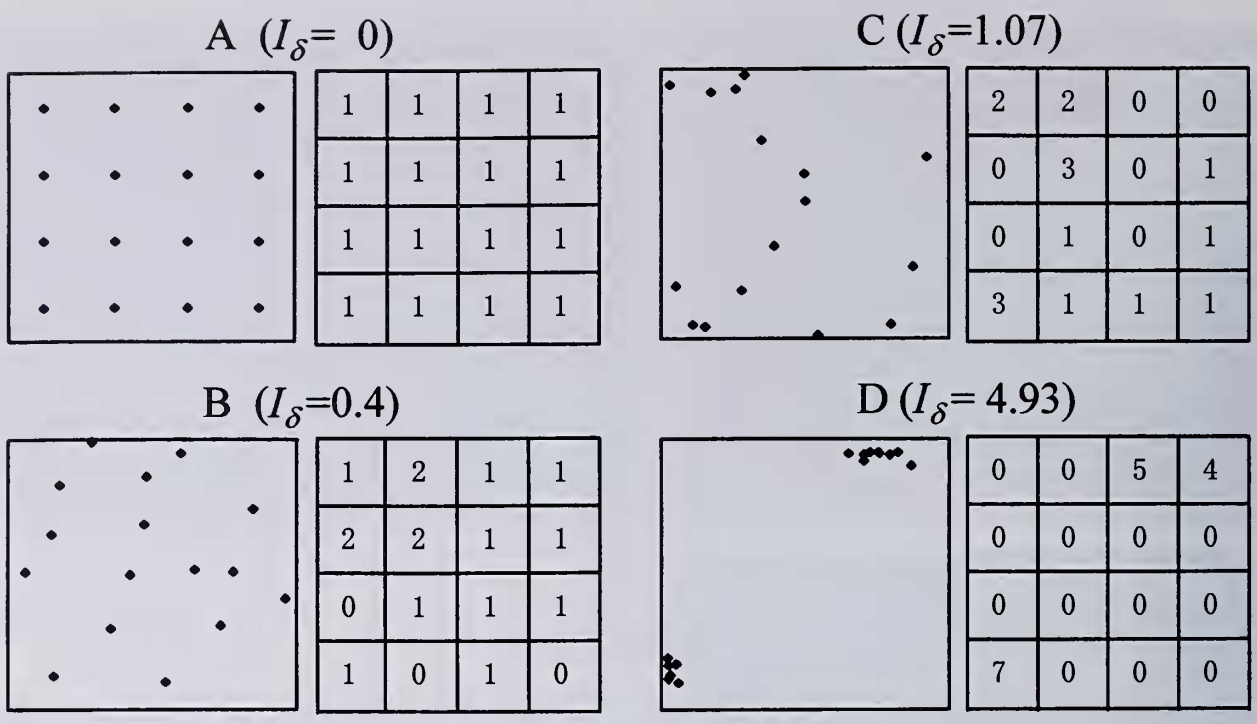

Figure 3. Effect of the spatial distribution pattern on the value of I_δ. In this figure, the area is divided into 16 contiguous squares each including a number of or no dots. **A**. Perfectly uniform distribution. **B**. Nearly uniform distribution. **C**. Random distribution. **D**. Considerably concentrated distribution.

within a single valve was not large enough to be significant. On the other hand, when the data from all species are combined, Q_s is negatively correlated with $\bar{S}$ at the 0.01 level of significance, both for simple prismatic and vertical composite prismatic shells (Figure 4A–B). This shows that variation in the size of prisms tends to decrease as prism size increases. The negative correlation between Q_s and $\bar{S}$ is clear especially in species with a simple prisms (Figure 4B), while the correlation is more or less obscure in species with vertical composite prisms (Figure 4A).

A positive correlation between I_δ and Q_s is found only in each specimen of *Unio biwae*, *Anodonta woodiana* and *Malleus regula* (Figure 4C, D). However, when all the data are combined, a positive correlation clearly emerges between I_δ and Q_s in species with vertical composite prisms (Figure 4C). In the case of species with simple prisms, Q_s is positively correlated with I_δ at the 0.05 level of significance, though the correlation is graphically unclear (Figure 4D). The positive relationship between I_δ and Q_s indicates that variation of the size of prisms tends to increase with increasing randomness of the distribution of nucleation sites.

Theoretical morphology

Growing circles model

To better understand the relationships between geometric features of prisms and the growth rate of each prism and/or of the net growth rate of the entire shell, the growth of aggregated prisms was modeled theoretically.

For modeling the process of microscopic growth, observing the initial growth stage of prisms helps understand the nature of crystal growth. Formerly, I reported that many small hemispherical incipient prisms occur on the inner surface of the periostracum at the growing margin in species possessing simple and vertical composite prisms (Ubukata, 1994, pl. 2, figs. 1–3). Consequently, a growing-circles model, which represents the growth of aggregated prisms, is introduced here.

Growth of a prismatic shell layer consists of three elements, namely, nucleation of prisms, growth of prisms, and accretionary growth of the entire shell. During a single short growth step, the mantle secretes calcium carbonate and nucleation of prisms occurs within the nucleation zone on the inner surface of a periostracum (Figure 5A). The periostracum subsequently secreted by the mantle edge pushes the earlier produced periostracum and its incipient prisms into a more proximal part of the shell (Saleuddin and Petit, 1983). After the prisms pass through the nucleation zone, prisms gradually grow and elongate, forming a columnar structure.

Let us consider hypothetical shell growth (Figure 5B). The accretionary growth of the entire shell during a short period of time is reflected in a shift of the nucleation zone. Growth of a prism is represented by the kinematics of an enlarging circle. Potential nucleation sites are distributed uniformly within a nucleation zone of width *h*. The distance between the potential nucleation sites can be expressed by *d*, which represents the size of a unit cell. Growth compo-

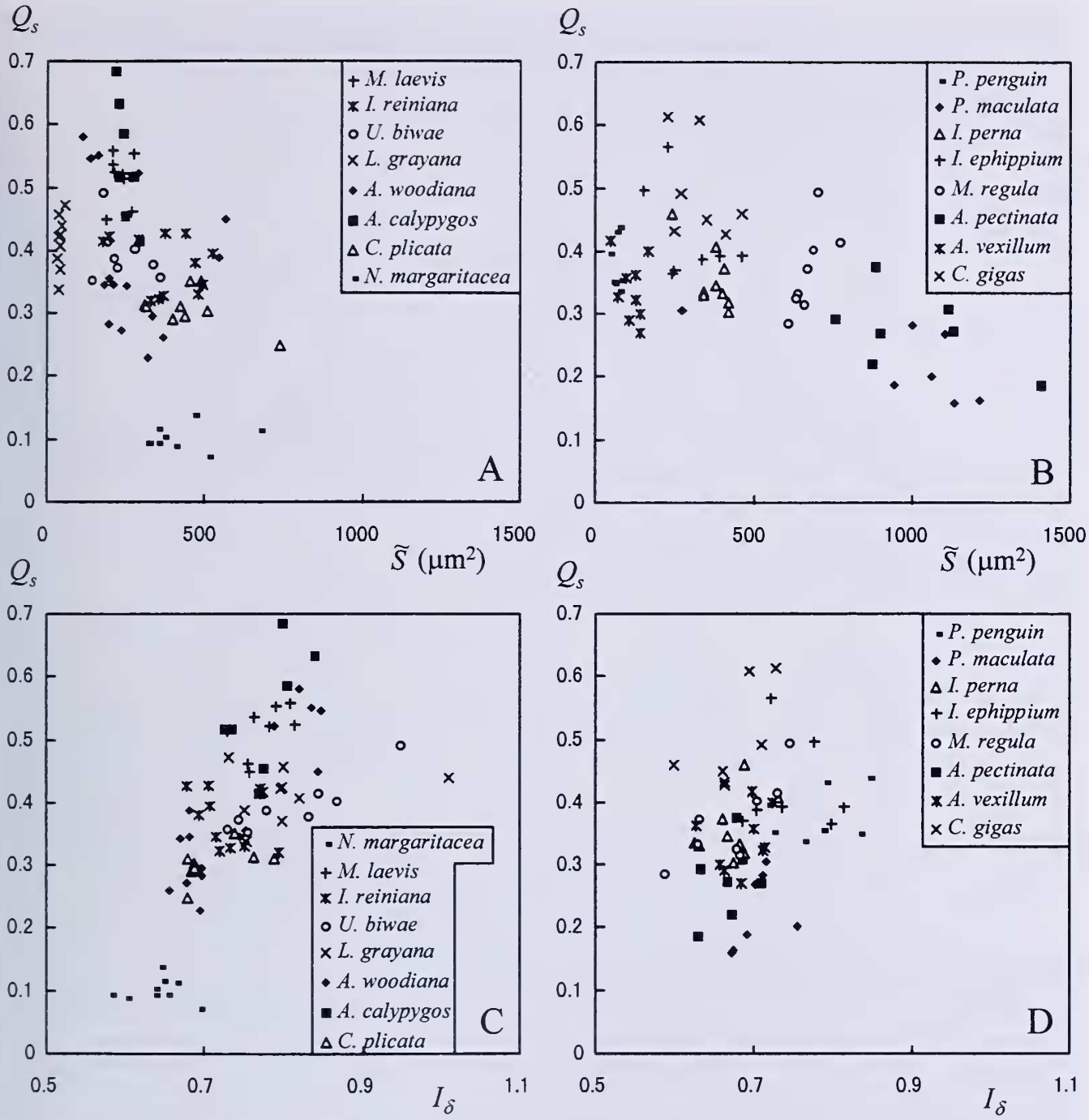

Figure 4. **A–B.** Relationship between $\tilde{S}$ and Q_s in actual shells. **A.** Data from species with vertical composite prisms. **B.** Data from species with simple prisms. **C–D.** Relationship between I_δ and Q_s for species with vertical composite prisms (**C**) and simple prisms (**D**).

nents are expressed as functions of growth stage s, rather than as functions of time, since the time scale of the growth process is difficult to ascertain in many cases. Over a period of one growth step, the mantle secretes a periostracum at the shell margin, giving rise to the stippled area in Figure 5B. If the growing margin of the shell shifts downward by d during the step, the growth step is regarded to be a unit interval of the growth. Then, the growth step Δs is generally defined as:

$$\Delta S \equiv \frac{\Delta l}{d}, \tag{3}$$

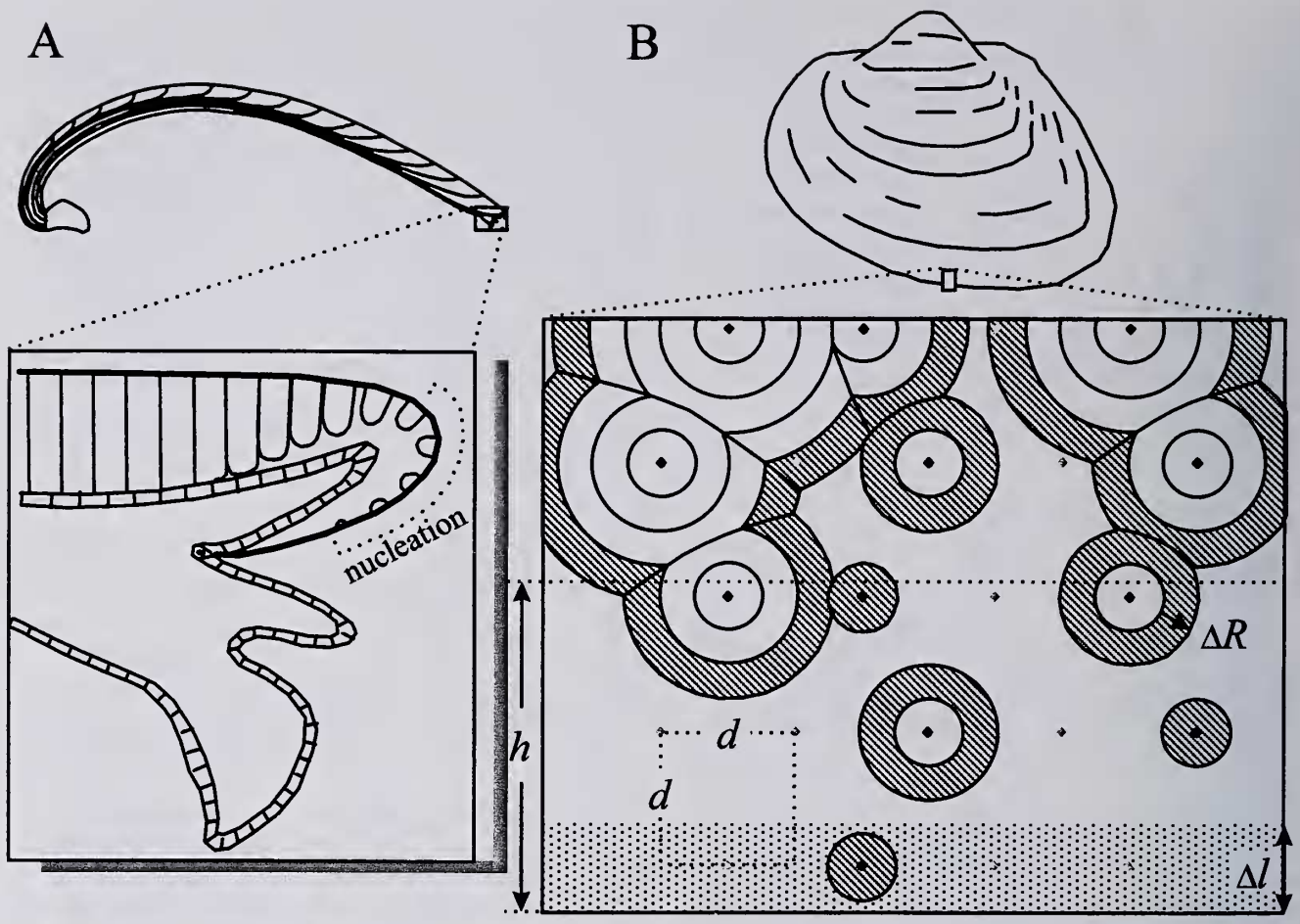

Figure 5. **A.** Schematic diagram of the radial section of the shell and mantle margin of a bivalve showing the position where nucleation of prisms occurs. **B.** The growing circles model. Black bold points indicate initiation sites of produced prisms, and gray ones potential nucleation sites of unborn prisms. During a given growth step Δs, the shell margin shifts by Δl (stippled area) and the radius of prisms increases by ΔR (shaded area). The dotted line indicates the dorsal limit of the nucleation zone.

where the growing margin of the shell shifts by Δl during the growth step.

Meanwhile, nucleation of a prism occurs at a potential nucleation site within the nucleation zone with a probability of q. Each prism is approximated by a circle which enlarges at a steady rate. During a growth step Δs, calcium carbonate precipitates along the circumference of each prism giving rise to a new additional rim shown by the shaded portion in Figure 5B, and the radius of each circle increases by ΔR. As the prisms grow, neighboring prisms come closer and finally in contact with one another, as a result forming a boundary between two prisms. Nucleation of prisms occurs randomly during each growth step, as a result of irregularity of the settling time among prisms. Consequently, a growing circle often occupies the space of nucleation and/or growth of a neighboring 'unborn' prism. A newborn prism sometimes loses in competition for space between neighboring prisms, and is geometrically terminated (Grigor'ev, 1965).

In the growing-circles model, growth of a shell and prisms is generally expressed by the following three parameters: C : the standardized growth rate of prisms, defined as the increase of the radius of a prism per growth step, normalized by size of a unit cell (d), P: probability of nucleation per growth step in each potential site, and L: the extent of the nucleation zone standardized by d. Probability of 'failure' of nucleation at each site per growth step is expressed as $1-P$, and the probability of failure of nucleation during a growth step Δs ($=1-q$) is obtained by raising $1-P$ to Δs^{th} power. Then, three growth parameters C, P and L are given by:

$$C \equiv \frac{\Delta R}{\Delta l},\ P \equiv 1-(1-q)^{\frac{1}{\Delta s}},\ L \equiv \frac{h}{d}. \tag{4}$$

Now, we can generally define a growth increment during an arbitrary growth step if three parameters C, P and L are given.

Computer simulation

In order to evaluate the effects of parameters C, P and L on the geometric pattern of prismatic structure, computer simulations were performed for growth of prisms based on

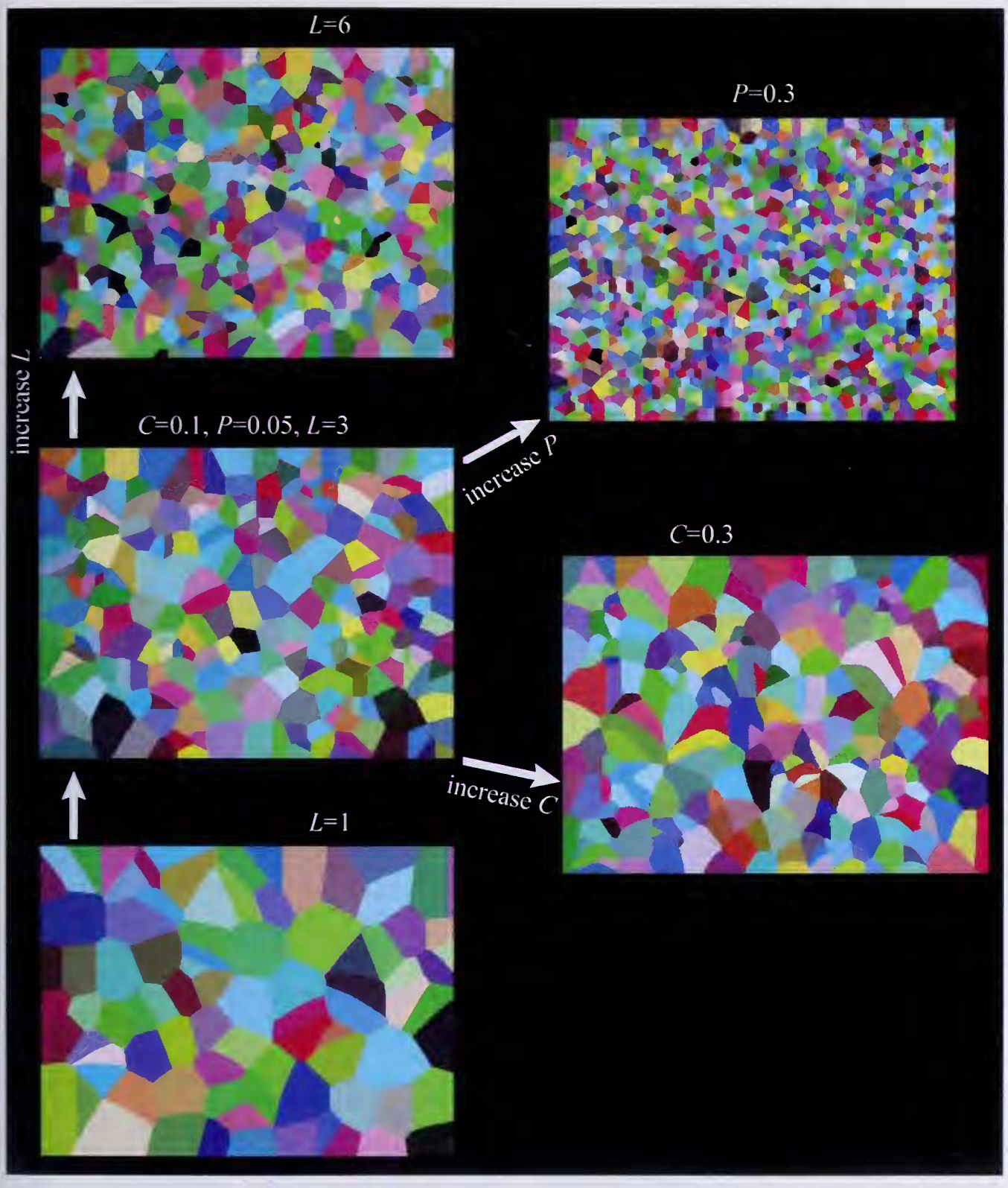

Figure 6. Color display of the growing circles model. Each prism is identified by its color. As C increases, size variation of the prisms also increases. As P or L increases, the median size of prisms tends to decrease.

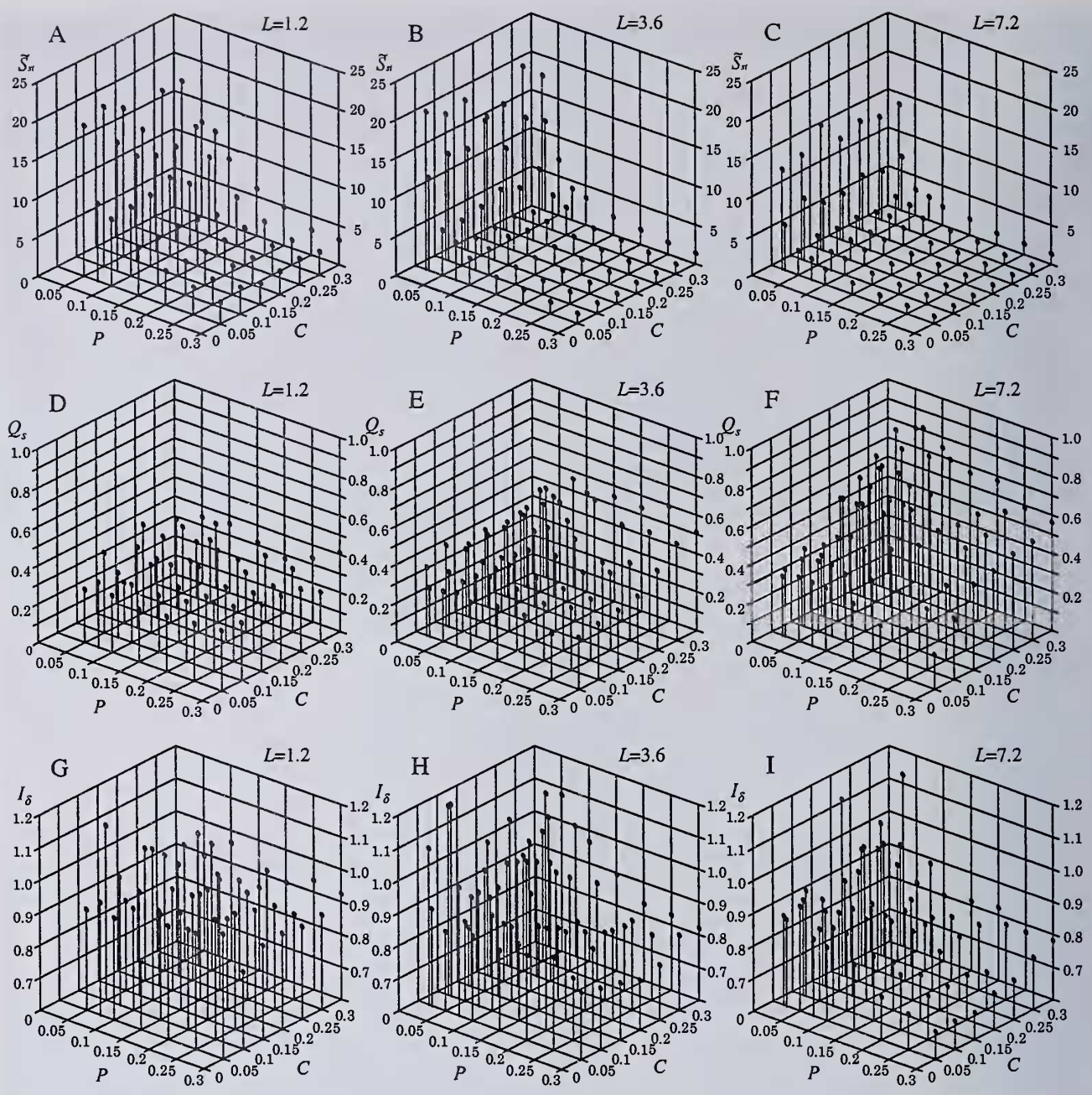

Figure 7. Three-dimensional block diagrams showing the relationships among growth parameters (C, P, L) and statistics $\tilde{S}$ (**A–C**), Q_s (**D–F**) or I_δ (**G–I**) on a C-P diagram at L values of 1.2, 3.6 and 7.2.

the growing-circles model. In the theoretical model, the area of a hypothetical prism was measured as the number of pixels (A) on the display surface, and both the standardized hinge spread (Q_s) and the median of a standardized area of hypothetical prisms ($\tilde{S}_{st}$) defined below were estimated in each model:

$$\tilde{S}_{st} \equiv \frac{\tilde{A}}{d^2}, \tag{5}$$

where $\tilde{A}$ is the median of A. The dimension of d is expressed as pixels on the computer. The coordinates of a nucleation site were recorded on each hypothetical prism for calculating the value of I_δ in a model. Computer simulations were carried out with a program written in VISUAL BASIC by means of a 64-bit workstation computer (Visual Technology VT-Alpha 600) interfaced with a CRT (Iiyama A702H).

Figure 6 shows a spectrum of geometric patterns of hypothetical prisms that were made by the growing circles model.

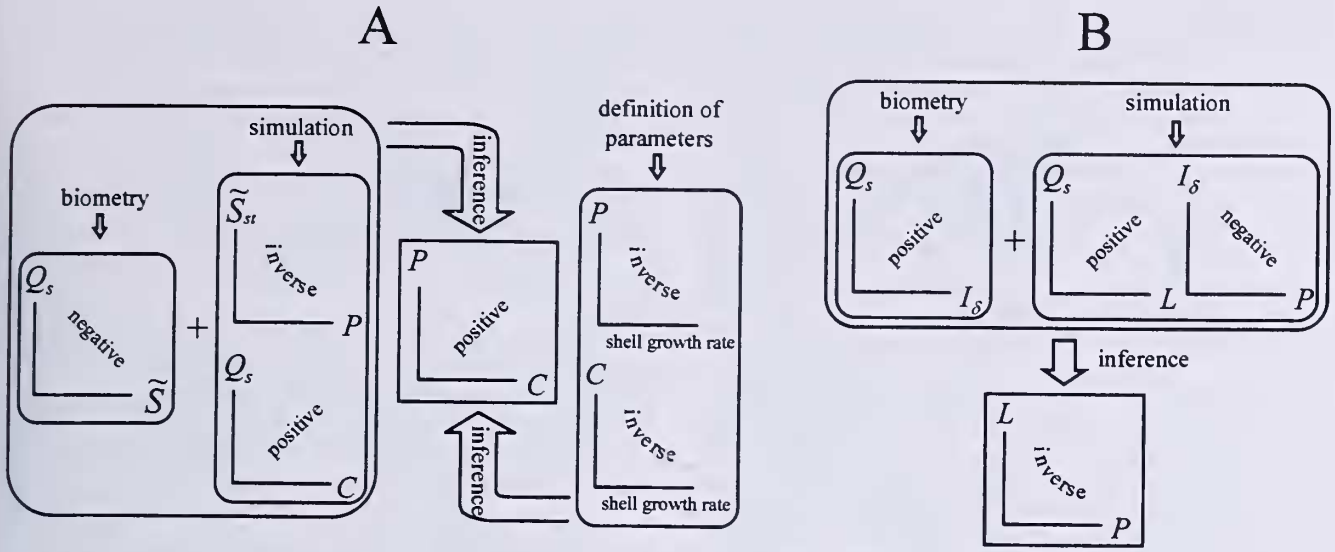

Figure 8. Summary of the biometric analyses and computer simulation. From coupling their results with the consequences from definition of the parameters, a relationship between growth parameters is inferred either in simple prisms (**A**) or composite prisms (**B**).

Each prism is identified by its color in a theoretical prismatic structure. If C is large, each prism grows considerably while it passes through the nucleation zone, as a result of the great irregularity of the birth time among prisms. Then, as C increases, the variation of prism size also increases. As P or L increases, the number of prisms increases while their size decreases.

Three-dimensional scatter diagrams illustrating the values of $\tilde{S}_{st}$ in relation to C and P, at L=1.2, 3.6 and 7.2 are given in Figure 7A–C, respectively. $\tilde{S}_{st}$, which means an 'average' prism size, seems to be inversely proportional to P, which represents the probability of nucleation. In addition, at the same combination of C and P, $\tilde{S}_{st}$ tends to increase as L decreases. This fact indicates that the size of hypothetical prisms increases as the nucleation zone becomes narrow.

Figure 7D–F is a series of diagrams showing the relationship among four parameters C, P, Q_s and L. When L is large enough, Q_s is positively correlated with C (Figure 7E, F). This fact suggests that variation of prism size tends to increase with increasing growth rate of prisms (ΔR in Eq.1) or with decreasing the accretion rate of the entire shell (ΔI in Eq.1). When L is small, no clear relationship exists between pairs of C, P and Q_s (Figure 7D). In a high C condition, Q_s at a given P also tends to increase with increasing L (Figure 7D–F).

Figure 7G–I shows the variation of I_δ in relation to C, P and L. When L is large, I_δ gradually decreases with increasing P. Since I_δ represents the degree of nonuniformity, this result indicates that the nucleation sites tend to be distributed uniformly as the probability of nucleation increases. In the high P region, I_δ at a given C decreases as L increases. This fact indicates that nucleation sites tend to be distributed randomly as the nucleation zone becomes narrower, when the probability of nucleation is high enough.

Geometric pattern and growth rate of prismatic shell

As mentioned above, the biometric analyses indicated a negative correlation between $\tilde{S}$ and Q_s especially in the species with simple prisms (Figure 4B), and the computer simulation predicted an inverse relationship between P and $\tilde{S}_{st}$ (Figure 7A–C) and also a positive correlation between C and Q_s (Figure 7E, F). To sum up these results, it can be predicted that P increases as C increases for those species with simple prisms (Figure 8A). That is also inferred from the definition of parameters. Since both P and C are inversely proportional to the growth rate of the entire shell, a positive correlation between C and P is quite reasonable (Figure 8A) if the size-frequency distribution of prisms is controlled mainly by the growth rate of the entire shell. Furthermore, even if both the growth rate of prisms and the probability of nucleation reflect the activity of mantle secretion, and if the size of prisms is controlled mainly by the activity of mantle secretion, the positive correlation between C and P is also expected.

Coupling of the biometrics and the simulation also suggests to us a relationship between the parameters P and L. The biometric analyses demonstrated a positive correlation between I_δ and Q_s, especially for species with vertical composite prisms as shown in Figure 4C. In addition, the computer simulation predicted a positive relationship between L and Q_s, and a negative correlation between P and I_δ as shown in Figure 7G–I. These two results suggest that P possibly decreases as L increases in species with vertical composite prisms (Figure 8B). Actually, an inverse relationship between L and P is expected if we assume that the frequency of nucleation per unit time interval is fixed.

To ascertain this prediction, relationships among simulated values of $\tilde{S}_{st}$, I_δ and Q_s were analyzed for each combina-

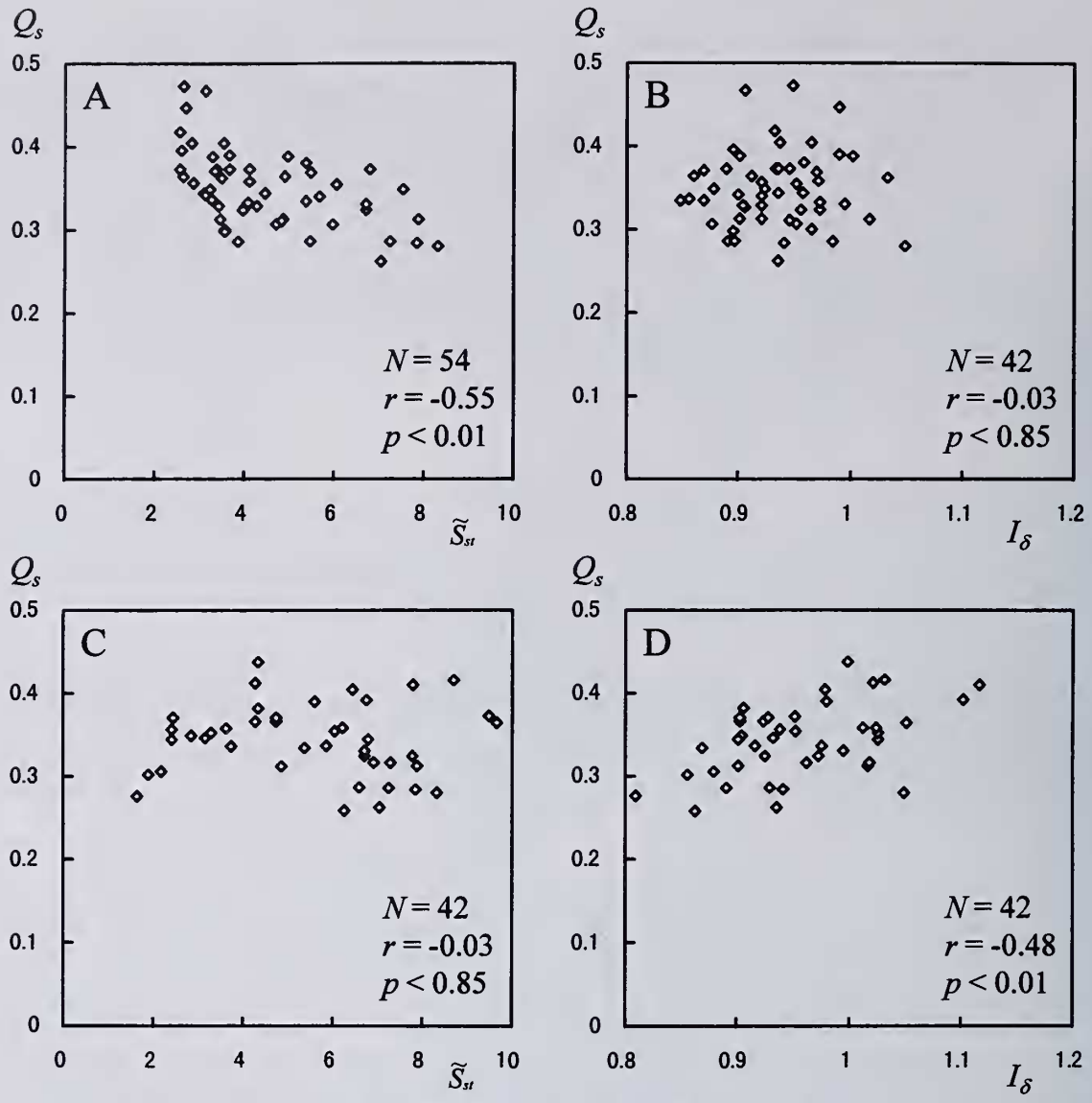

Figure 9. Relationships between $\tilde{S}_{st}$ and Q_s and between I_δ and Q_s when three parameters satisfy equations as follows: $C=aP$, $P=b/L$, where a and b are coefficients. N represents the total number of samples examined, r exhibits the correlation coefficient, and p is the significance level of the correlation. **A–B**. a=3, $0.05 \leq b \leq 0.175$. **C–D**. $1 \leq a \leq 3$, b=0.05.

tion of C, P and L, when a positive correlation between C and P and an inverse relationship between L and P are assumed, as in the following relations:

$$C = aP,\ P = \frac{b}{L}, \tag{6}$$

where a and b are coefficients. Computer simulations were performed under the following conditions: 1) a is fixed to 3, and b varies between 0.05 and 0.175, 2) a varies between 1 and 3, and b is fixed to 0.05. Figure 9 is a diagram showing the relationships between $\tilde{S}_{st}$ and Q_s and between I_δ and Q_s.

The results of the simulations under a fixed value of a (=3) and various values of b show a negative correlation between $\tilde{S}_{st}$ and Q_s (p<0.01, Figure 9A), but do not indicate any linear relationship between I_δ and Q_s (Figure 9B). Under even this condition, a negative correlation between $\tilde{S}_{st}$ and Q_s and a positive correlation between I_δ and Q_s were approached by a multiple regression analysis, which shows a significant trend for Q_s to increase as a function of - $\tilde{S}_{st}$ and I_δ:

$$Q_s^* = -0.573\tilde{S}_{st}^* + 0.128\, I_\delta^* \quad (r=0.565,\ F=11.94,\ p<0.01),$$

where Q_s^*, S_{st}^* and I_δ^* are standardized variables of Q_s, $\tilde{S}_{st}$ and I_δ, respectively. In this case, a negative relationship between $\tilde{S}_{st}$ and Q_s is especially prominent. This relationship, concordant with that of the biometric analyses as shown in Figure 4B, D, strongly supports conspicuous posi-

tive correlation between C and P assumed as in the Eq. 6, particularly for simple prisms. As stated above, a positive correlation between C and P suggests that both prism size and its variation are mainly controlled either by the growth rate of the entire shell, or by the activity of mantle secretion. If the former is the case, simple prisms must tend to be uniformly large as the entire shell grows faster. On the other hand, if the latter is the case, density of nucleation and growth rate of prisms both must decrease as the secretive activity of the mantle decreases, and a negative relationship is expected between size and the growth rate of simple prisms.

On the other hand, the results of computer simulations with various values of the coefficient a and the fixed coefficient b (=0.05) show a positive correlation between I_δ and Q_s (p<0.01, Figure 9D), but no significant relationship between $\tilde{S}_{sv}$ and Q_s (Figure 9C). A multiple regression analysis for Q_s on $\tilde{S}_{sv}$ and I_δ provides a significant trend to increasing Q_s as a function of $\tilde{S}_{sv}$ and I_δ:

$$Q_s^* = -0.393\tilde{S}_{sv}^* + 0.686\, I_\delta^* \quad (r=0.582,\ F=9.99,\ p<0.01).$$

In this equation, a positive relationship between I_δ and Q_s is more striking than a negative relationship between $\tilde{S}_{sv}$ and Q_s. This is concordant with the results of the biometric analyses in species with vertical composite prisms shown in Figure 4A, C. This fact supports the assumption that P has an inverse relationship with L as defined in Eq. 6, particularly in vertical composite prisms. This assumption implies that the number of nucleations per unit time interval is fixed to a constant value. In the species having a large nucleation zone, in which the value of L is large, maintenance of the probability of nucleation inevitably causes a large number of nuclei. If we assume an upper limit of the total number of nuclei per unit time interval, the probability of nucleation will vary inversely with the width of the nucleation zone. If the total number of nuclei per unit time interval is fixed, the density of nucleation is expected to decrease as the total shell grows faster. In this case, the median size of prisms is controlled mainly by the growth rate of the entire shell. This fact suggests that, in the case of vertical composite prisms, prism size tends to increase as the entire shell grows faster.

Discussion and conclusion

Wada (1961) studied the size of crystals in a nacreous shell layer of *Pinctada martensii* in relation to the rate of calcium carbonate deposition. He demonstrated that when the rate of shell deposition is at a maximum, a large number of small crystals occurs on all the nacreous surfaces, while larger crystals occur as the rate of deposition decreases. In addition, Wada (1972, 1985) also reported an inverse relationship between them for such bivalves as *Pinctada fucata*, *Pinna attenuata* and *Hyriopsis schlegeli*. Wada assumed that the primary factor determining size of crystals was the degree of calcium carbonate concentration in the extrapallial fluid. He regarded the rate of calcium carbonate deposition as the rate of crystal growth, and thought that larger crystals tend to grow slowly at a low degree of supersaturation of the fluid, at which the frequency of nucleation diminishes. The results of the present study may partly support those of Wada, since the negative correlation between size and growth rate of crystals is also expected in this study if the size of prisms is assumed to be controlled by the activity of mantle secretion.

Unlike prismatic structure, nacreous structure does not form the outermost shell layer in bivalves. In the nacreous layer, deposition corresponds to thickening of the shell or growth of crystals, rather than growth of the entire shell. Therefore, the size of crystals in the nacreous layer correlates with the rate of crystal growth rather than with the growth rate of the entire shell. On the contrary, the net growth rate of the entire shell, which reflects the growth rate of the soft parts, seems to be significant for the size of crystals which constitute the outermost shell layer.

Ubukata (1994) claimed that relatively rapid growth of prisms produces prisms prominently inclined to the outer shell surface, because of retardation of the initiation of their forward growth relative to the radial direction. Although such inclined prisms are commonly found in species belonging to Unionidae and Ostreidae (Ubukata, 1994), their prisms also characteristically fell in low (small size) and high Q_s (irregular in size) regions in Figure 4A, B (refer to Table 1 for higher taxonomy). The present study suggests that such a pattern is produced under the condition of either rapid growth of prisms or slow growth of the entire shell. Ubukata (1994) demonstrated that the relative growth rate of prisms to that of the entire shell determines the orientation of elongation of the prisms.

This study suggests that the sizes of prisms and their size variability correlate with the growth rate of the shell in bivalves. It is well known that internal microgrowth increments often provide a high-resolution record of growth rate and physiological condition of a bivalve (Lutz and Rhoads, 1980), particularly in species with crossed lamellar and horizontal composite prismatic shells. In simple prismatic and vertical composite prismatic shells, however, it is hard to estimate the growth rate of the shell from an analysis of internal microgrowth increments, because periodic growth increments tend to be obscure. The size-frequency distribution of prisms may be a promising index for estimating the growth rate of a fossil bivalve shell.

This study indirectly estimates the relationship between the size of prisms and the growth rate of the shell or prisms from computer simulations, but the direct observation of the growth rate of the shell or prisms remains to be performed. An experimental study on growth of a shell and/or crystals may be required for clarifying the relationship between the crystal size and the growth rate more clearly, and for obtaining a regression equation to predict the growth rate from prism size. The growth rate of the shell and/or crystals is clearly related to the physiological condition of a fossil organism, and has the potential to in spire a research field of 'paleophysiology'.

Acknowledgments

I thank Enrico Savazzi (Uppsala University), Kazushige Tanabe (University of Tokyo), Rihito Morita (Natural History Museum and Institute, Chiba) and Joseph G. Carter (University of North Carolina) for critical review of the manu-

script and for valuable comments. This study has been supported by Grant-in-Aid for Scientific Research (A) from the Japan Society for the Promotion of Science (No. 10304040).

References

Carter, J. G. and Clark, G. R. II, 1985: Classification and phylogenetic significance of molluscan shell microstructure. *In*, Broadhead, T. W. *ed.*, *Mollusks: Notes for a Short Course*, p. 50-71. *Department of Geological Sciences, Studies in Geology*, 13. University of Tennessee, Knoxville.

Carter, J. G., Bandel, K., de Buffrénil, V., Carlson, S. J., Castanet, J., Crenshaw, M. A., Dalingwater, J. E., Francillon-Vieillot, H., Géraudie, J., Meunier, F. J., Mutvei, H., de Ricqlès, A., Sire, J. Y., Smith, A. B., Wendt, J., Williams, A. and Zylberberg, L., 1990: Glossary of skeletal biomineralization. *In,* Carter, J. G. *ed.*, *Skeletal Biomineralization*: *Patterns*, *Processes and Evolutionary Trends*, vol. 1, p. 609-671. Van Nostrand, New York.

Grigor'ev, D. P., 1965: *Ontogeny of Minerals*, 250p. Israel Program for Scientific Translations Ltd., Jerusalem.

Hoel, P. G., 1976: *Elementary Statistics*, 4th ed., 361p. John Wiley and Sons, Inc., New York.

Lutz, R. A. and Rhoads, D. C., 1980: Growth patterns within the molluscan shell. An overview. *In,* Rhoads, D. C. and Lutz, R. A. *eds.*, *Skeletal Growth of Aquatic Organisms*, p. 203-254. Prenum Press, New York.

Morisita, M., 1959: Measuring of dispersion of individuals and analysis of the distributional patterns. *Memoirs of the Faculty of Science*, *Kyushu University*, Series E, vol. 2, p. 215-235.

Saleuddin, A. S. M. and Petit, H. P., 1983: The mode of formation and the structure of the periostracum. *In,* Saleuddin, A. S. M. and Wilbur, K. M. *eds.*, *The Mollusca*, vol. 4, *Physiology*, pt. 1, p. 199-234. Academic Press, New York.

Ubukata, T., 1994: Architectural constraints on the morphogenesis of prismatic structure in Bivalvia. *Palaeontology*, vol. 37, p. 241-261.

Ubukata, T., 1997a: Microscopic growth of bivalve shells and its computer simulation. *The Veliger*, vol. 40, p. 165-177.

Ubukata, T., 1997b: Mantle kinematics and formation of commarginal shell sculpture in Bivalvia. *Paleontological Research*, vol. 1, p. 132-143.

Ubukata, T., 2000: Theoretical morphology of composite prismatic, fibrous prismatic and foliated shell microstructures in bivalve. *Venus*, vol. 59, p. 297-305.

Wada, K., 1961: Crystal growth of molluscan shell. *Bulletin of the National Pearl Research Laboratory*, vol. 7, p. 703-828.

Wada, K., 1972: Nucleation and growth of aragonite crystals in the nacre of bivalve molluscs. *Biomineralization*, vol. 6, p. 141-159.

Wada, K., 1985: Growth of $CaCO_3$ crystals in bivalve shell mineralization. *Journal of the Japanese Association for Crystal Growth*, vol. 12, p. 57-70. (*in Japanese with English abstract*)